Role of side-chain interactions on the formation of α-helices in model peptides

Farbod Mahmoudinobar,[1] Cristiano L. Dias,[1,*] and Ronen Zangi[2]
[1]*New Jersey Institute of Technology, Physics Department, University Heights, Newark, New Jersey, 07102-1982, USA*
[2]*Department of Organic Chemistry I and POLYMAT, University of the Basque Country UPV/EHU, Avenida de Tolosa 72, 20018, San Sebastian, Spain IKERBASQUE, Basque Foundation for Science, Maria Diaz de Haro 3, 48013 Bilbao, Spain*
(Received 3 January 2015; published 25 March 2015)

The role played by side-chain interactions on the formation of α-helices is studied using extensive all-atom molecular dynamics simulations of polyalanine-like peptides in explicit TIP4P water. The peptide is described by the OPLS-AA force field except for the Lennard-Jones interaction between C_β–C_β atoms, which is modified systematically. We identify values of the Lennard-Jones parameter that promote α-helix formation. To rationalize these results, potentials of mean force (PMF) between methane-like molecules that mimic side chains in our polyalanine-like peptides are computed. These PMF exhibit a complex distance dependence where global and local minima are separated by an energy barrier. We show that α-helix propensity correlates with values of these PMF at distances corresponding to C_β–C_β of $i - i + 3$ and other nearest neighbors in the α-helix. In particular, the set of Lennard-Jones parameters that promote α-helices is characterized by PMF that exhibit a global minimum at distances corresponding to $i - i + 3$ neighbors in α-helices. Implications of these results are discussed.

DOI: 10.1103/PhysRevE.91.032710 PACS number(s): 87.14.ef, 87.15.A−, 87.15.bd

I. INTRODUCTION

α-helices and β-sheets are the main building blocks of protein structures serving as a template for almost 50% of all residues [1]. These motifs are also present in the structure of intrinsically disordered and amyloid peptides in which stacking of β-sheets has been related to diseases such as Alzheimer's and Parkinson's [2–4]. Due to their ubiquitous presence, α-helices and β-sheets have been the subject of numerous studies aiming to understand the molecular forces driving their formation. However, this remains a topic of debate as intra-backbone hydrogen bonds (which were initially thought to account for α-helices and β-sheets [5–7]) might not be significantly favorable to drive this process in aqueous solution [8–13]. As a result, most algorithms designed to predict the propensity of secondary structures are knowledge based [14]. The aim of the current paper is to provide insights into the forces driving the formation of α-helices and, in particular, the role played by the effective interactions between side chains.

Since the seminal work of Kauzmann, hydrophobic interactions are believed to be main ingredients determining native protein structures [8,9,15]. They emerge because nonpolar regions of proteins or peptides tend to minimize their solvent exposed area accounting for the globular shape that characterizes the native state. The importance of these hydrophobic interactions can be inferred from the positive curvature of the Gibbs free energy of unfolding with respect to temperature [8,16,17]. This is typical of nonpolar solvation [18–21], and it rationalizes cold denaturation of proteins [16,22,23]. Also, the diversity of native structures can only be encoded in the amino acid sequence (not in the backbone), suggesting that side-chain properties and, in particular, the burial of nonpolar residues in the dry protein core is responsible for folding. Accordingly, after the first protein structure was resolved experimentally, its dry core was observed to be made mostly of nonpolar residues [24,25]. Secondary structures form during folding because the polar backbone is also buried in the dry protein core accounting for an enthalpic penalty that can be minimized through the formation of intrabackbone hydrogen bonds. This favors internal organizations within the collapsed state such that α-helices and β-sheets emerge in proteins to avoid the enthalpic penalty of burying the backbone in the dry core. In contrast to this process, peptide structures do not exhibit a dry core suggesting that the mechanism for forming secondary structures could differ from the one in globular proteins. This is supported by experiments showing that destabilization of α-helices by cosolvents that form hydrogen bonds correlate with the strength of these bonds for peptides but not for proteins [9]. In addition, very small concentrations of surfactants are sufficient to unfold proteins efficiently [26], whereas they do not destabilize helices [27]. Despite these insights, it is still not clear what drives α-helices and β-sheets in peptides.

Propensities to form α-helices were first attributed to the restriction of the configurational entropy of side chains upon folding [28,29]. However, a poor correlation between the reduction in the side-chain entropy and helix propensity was found [30], putting into question the validity of this argument [31]. The possibility that helix propensities are modulated by energy was first proposed by Luo and Baldwin, who used thermal unfolding curves of five nonpolar amino acids in water-trifluoroethanol mixtures [32]. This was then extended by Makhatadze and coworkers, who used calorimetric measurements of folding a model host peptide in which the helix formation is induced by metal binding [31,33]. This concept has been further developed in the prediction of the helical behavior of peptides. Here, experimental data were used to parametrize empirically a set of energy contributions for every side chain [34]. In fact, modulating side-chain interactions have been exploited in designing very short helical peptides in solution such as in the 5-mer peptide $WAAAH^+$ where strong cation-π interaction is established between $i - i + 4$ neighbors [35]. In a computational study, side-chain interactions were reported to play an important role

*cld@njit.edu

in transitions from α-helix to β-sheet in a short polyleucine peptide [36]. Furthermore, in the AGADIR algorithm to predict α-helix content [35], the inclusion of side-chain interactions was particularly relevant since, without them, natural amino-acid sequences tend to lack measurable helix content in water [37].

It should be noted that when taking into account side-chain contributions in promoting secondary structures, the important quantity to consider is the *effective* interaction of the side chain with the other groups of the peptide. This is particularly relevant in aqueous solutions where water increases the complexity of energy landscapes of molecular interactions. For example, the interaction between methane molecules in water (which are often used as a model for the interaction of nonpolar side chains [38–41]) is characterized by a global and a local minimum at short ($\sim$3.8 Å) and intermediate ($\sim$7 Å) distances, respectively, separated by an energy barrier related to desolvation effects (at $\sim$5.7 Å) [42]. These features affect short range structures in proteins and peptides. For example, in peptides made from aliphatic amino acids it was shown that distances between C_β–C_β atoms of $i-i+3$ and $i-i+4$ neighbors coincide with the position of desolvation barriers, while C_β–C_β distances of $i-i+2$ neighbors in β-sheets coincide with the local minimum [22,43–45]. This was shown to play an important role in the propensity of secondary structures studied computationally with implicit water models [45].

In the current paper, we study how the effective potential between side-chains affects the probability to form α-helices using all-atom molecular dynamics simulations in explicit water. To that purpose we use polyalanine-like peptides described by the OPLS-AA force field where the Lennard-Jones interactions between C_β atoms are modified. We change both the equilibrium Lennard-Jones distance, σ, and the well depth, ϵ. In addition, we also compute potentials of mean force (PMF) for the interaction of methane-like molecules that represent side-chain groups in the polyalanine simulation. We find a good correlation between the propensity to induce α-helical conformations in peptides and the effective interactions between the side chains (computed from the PMF of methane-like molecules). In particular, greater propensities are observed when the PMF of methane-like molecules exhibit a minimum at distances corresponding to C_β distances in α-helices.

II. METHODS

We model 9- and 12-residue homogeneous (uncharged) peptides deprotonated at the N-terminal and protonated at the C-terminal using the OPLS-AA force field. Peptides are polyalanine chains in which the σ parameter of the Lennard-Jones (LJ) potential between C_β atoms is varied systematically from 0.27 nm to 0.57 nm in steps of 0.10 nm in the different simulations. Since the original LJ parametrization of polyalanine is $\sigma = 0.35$ nm and $\epsilon = 0.276144$ kJ/mol, we also perform simulations using these values as well as $\sigma = 0.45$ nm and $\epsilon = 0.276144$ kJ/mol. All other atoms of the peptides were represented by the OPLS-AA force field including the three hydrogen atoms attached to each C_β [46–49]. The interaction between C_β and any other atom in the system (excluding other C_β's) corresponds to that of polyalanine.

The simulation box consists of a 9-mer or a 12-mer peptide solvated in 1535 or 1681 TIP4P water molecules [50], respectively. Bond distances and angles within water molecules are constrained using the SETTLE algorithm [51], whereas covalent bonds within the peptide are constrained using the LINCS algorithm [52]. Starting with fully extended polyalanine configurations (generated using the program WHATIF [53]), the system is relaxed by a 100 ps molecular dynamics simulations (with $\epsilon_{C_\beta - C_\beta} = 0.0$ kJ/mol) yielding extended random coil conformations. These structures are used as starting configurations in our simulations. Within each peptide length, we use the same starting configurations for simulations with the different σ and ϵ parameters.

Each trajectory was propagated for 400 ns, whereas results for $\epsilon = 0.47$ nm and $\epsilon = 1$ kJ/mol were taken from a previous study [54]. Atomic positions of the peptide were saved every 10 ps, and they were used in all analyses. Note that a recent computational study of hepta-alanine modeled using the OPLS-AA force field and compared with NMR-derived J-coupling constants reported convergence of the value of χ^2 within the first 250 ns of the trajectory [55].

The molecular dynamics package GROMACS version 4.5.4 [56] was used to perform all simulations using a time step of 2 fs. Electrostatic forces were evaluated using the Particle-Mesh Ewald method [57] (real-space cutoff of 1.2 nm, grid spacing of 0.12 nm, and quadratic interpolation), while a cutoff of 1.2 nm was used for LJ forces (with long-range dispersion correction for the energy and pressure). The entire system was maintained at a constant temperature of 300 K using the velocity rescaling thermostat [58] and a coupling time of 0.1 ps. Pressure was kept fixed at 1.0 bar using the Berendsen thermostat [59] with a compressibility of 5×10^{-5} bar^{-1} and a coupling time of 1.0 ps.

To estimate the effective interactions between two C_β atoms within the peptide chain we calculated the potential of mean force (PMF) between methane-like molecules in solution. PMF were computed using the λ-coupling approach with a series of 51 λ-points from 0.00 to 1.00. At every λ-point the distance between carbon atoms of the two methane-like molecules was constrained to a specified value and the system simulated for 4.0 ns. The average force (over 3.5 ns data collection step) needed to satisfy this constraint, thus, $\langle \partial \mathcal{H}/\partial\lambda \rangle$, was then integrated as a function of λ to obtain the PMF. As the PMF represents only relative values, the resulting curve was shifted such that the value at $\lambda = 1.00$ was equal to zero. In these free energy simulations the carbon-hydrogen bonds were described by harmonic potential, and therefore, the time step of the simulations was reduced to 0.001 ps. Because each OPLS-AA hydrogen carried a charge of $+0.06\,e$ the carbon atom of the methane-like molecule was assigned a charge of $-0.24\,e$.

III. RESULTS

A. Side-chain interactions

In Fig. 1 we study how the σ parameter of the LJ interaction between C_β atoms affects the formation of secondary structures using fixed $\epsilon = 1$ kJ/mol. For all values of σ, residues

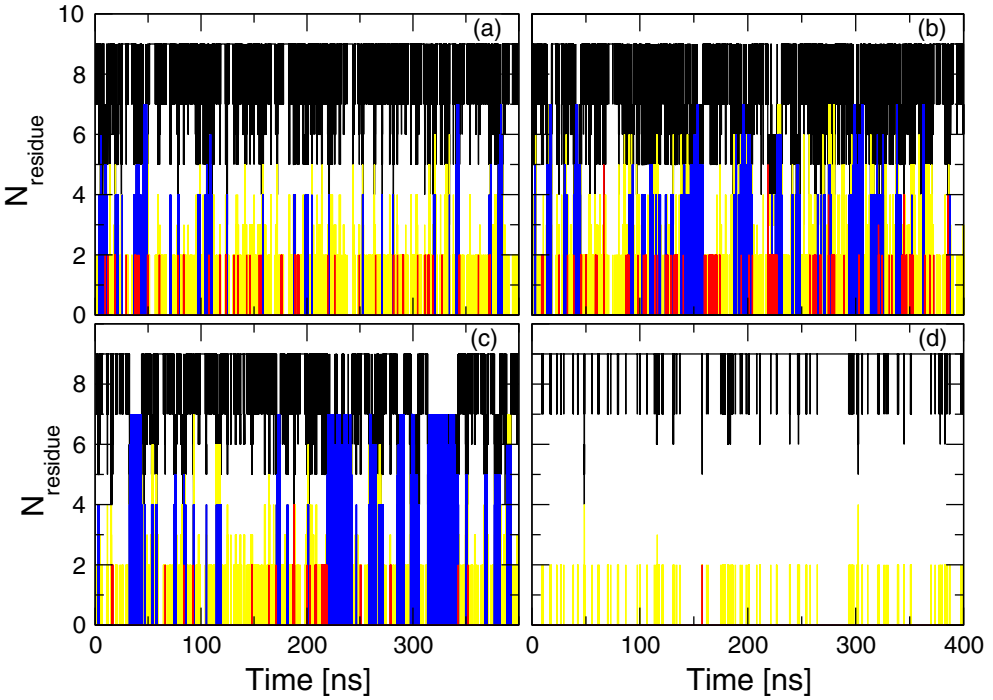

FIG. 1. (Color online) Time evolution of secondary structure content for $\epsilon = 1$ kJ/mol, N = 9, and σ values of (a) 0.27 nm, (b) 0.37 nm, (c) 0.47 nm, and (d) 0.57 nm. N_{residue} is the number of residues assuming coil in black, β-sheet in red (medium gray), turn in yellow (light gray), and α-helix in blue (dark gray) structures.

of the peptide spend most of their time in coil conformations. This is particularly striking for $\sigma = 0.57$ nm [Fig. 1(d)] in which case ordered structures (α-helix and β-sheet) are not observed in the time frame of the simulation and the peptide spends 94% of the time in coil conformations.

Ordered secondary structures, mostly α-helices and turns, are observed only for σ values smaller than 0.57 nm. From Fig. 1, it seems that turns are more prominent for $\sigma = 0.37$ nm (panel b), whereas populations of α-helix seem to occur more frequently for $\sigma = 0.47$ nm (panel c). These

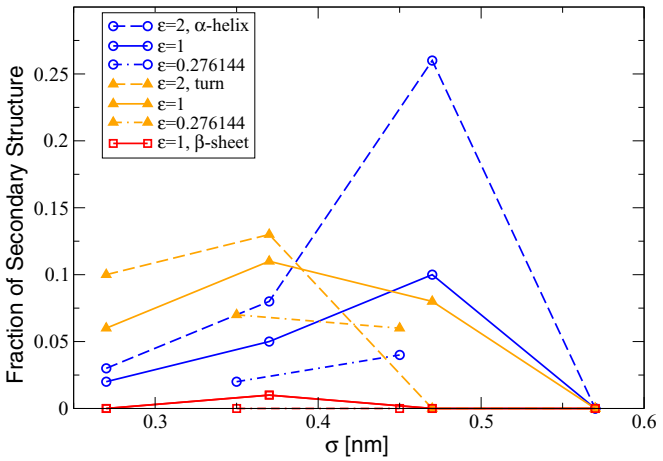

FIG. 2. (Color online) Content of various secondary structure elements as a function of σ for several values of ϵ. All plots are for the nine-residue-long peptides ($N = 9$) averaged over the entire 400 ns trajectory. Helices are depicted in blue (open circles), turns in orange (triangles), and β-sheets in red (square).

observations are quantified in Fig. 2, where we show the average content of secondary structures as a function of σ for different ϵ values. It confirms that the largest content of turn occurs for $\sigma = 0.37$ nm, whereas α-helix content peaks at $\sigma = 0.47$ nm. In our simulations, the formation of β-sheet structures is negligible with a maximum content of $\sim$1% occurring at $\sigma = 0.37$ nm. However, the lack of β-sheet content observed in this study is expected because lengths of our peptides are relatively short, rendering the penalty for loop formation large compared to the stabilization obtained from the interaction between the strands. This penalty can be reduced by incorporating specific sequences in the middle of the chain (e.g., sequences containing proline) that favor turns [60,61]. Accordingly, NMR experiments have reported that the combination of turn propensity and side-chain interactions in β-strands are required to form stable β-hairpins is short peptides [62].

In Fig. 2 we also study how the strength of the ϵ parameter of the LJ interaction affects secondary structure formation.

For σ values smaller than 0.57 nm, we observe an increase in α-helix content with increasing ϵ. This is in agreement with previous studies showing that interactions between side chains can modulate α-helix formation [31–33,45,54]. The population of turns has a more complex behavior in the parameter space we are exploring. At fixed $\sigma = 0.37$ nm, the content of turns increases with increasing ϵ, whereas at fixed $\sigma = 0.47$ nm the percentage of turn structures drops drastically from $\sim$10 % at $\epsilon = 1$ kJ/mol to zero at $\epsilon = 2$ kJ/mol. This abrupt reduction in the content of turns coincides with a large increase ($\sim$15 %) in the population of α-helices suggesting that increasing ϵ from 1 kJ/mol to 2 kJ/mol at fixed $\sigma = 0.47$ nm could trigger a turn-to-helix transition. Note that according

TABLE I. Secondary structure content averaged over 400 ns using $\epsilon = 1.0$ kJ/mol.

	$\sigma = 0.37$ nm			$\sigma = 0.47$ nm		
N	% helix	% turn	% coil	% helix	% turn	% coil
9	5	11	63	10	8	65
12	7	11	56	44	9	38

to DSSP definitions, a residue is assigned to a turn whenever the CO– group of residue i forms a hydrogen bond with the NH– group of residue $i+n$ where $n = 3$, 4, or 5, while a residue is assigned to an α-helix whenever two (or more) consecutive residues form turns with $n = 4$. Thus, a structure determined as a turn according to the definitions of DSSP might not be too different from an α-helix, and thus an increase in ϵ at fixed $\sigma = 0.47$ nm (which is a length-scale that favors C_β–C_β interactions in α-helix) could indeed trigger turn-to-helix transitions.

B. Peptide length

Experimentally, the formation of secondary structures in polyalanine has been shown to depend on peptide length. In particular, α-helix content was reported to increase with peptide length up to $N = 19$, whereas larger chains ($19 < N < 25$) were shown to aggregate into oligomers [63]. End effects in α-helices, involving the first and last three residues (in addition to capping groups at the N- and C-termini), contribute to this dependence because only one intrabackbone hydrogen bond is formed in these residues as opposed to two for residues in the middle of the helix. In the same vein, side-chain atoms form less interactions in these residues compared to the ones in middle of the helix. As a result, end effects are more pronounced in short compared to long peptides, and they involve 2/3 and 1/2 of the residues in 9- and 12-mer chains, respectively.

To test how changes in side-chain interactions affect peptides of different lengths, we perform a set of simulations using peptides made of 12 residues ($N = 12$). In Table I they are compared with the 9-mer simulations performed in the previous section.

Turn content is not strongly affected by peptide length: changing peptide length from 9 to 12 residues increases the percentage of turn by 0% for $\sigma = 0.37$ nm and by 12% for $\sigma = 0.47$ nm. In contrast, α-helix content is strongly dependent on peptide length; for $\sigma = 0.37$ nm, the percentage of α-helical structures increases by 40% with increasing N, and for $\sigma = 0.47$ nm it increases by 340%.

Time dependence of assigned secondary structures based on DSSP to residues along the amino acid sequence is shown in Fig. 3.

For $\sigma = 0.37$ nm (panel a), five α-helix nucleating events involving at least four residues are observed within the simulation time. For $\sigma = 0.47$ nm (panel b), there is only one main α-helix nucleating event with a life time of ~300 ns, although several structural transitions involving a complete and partial α-helices are observed.

Notice that in an α-helix, the number and the energy of intrabackbone interactions change by the same amount when the peptide length increase from 9 to 12 residues for $\sigma = 0.37$ nm and 0.47 nm. The number of side-chain interactions also increases by the same amount for $\sigma = 0.37$ nm and 0.47 nm but not the energy of these interactions. Thus, in our simulations (see Table I) the 40% increase in α-helix content (when the length of the peptide increases from 9 to 12 residues) for $\sigma = 0.37$ nm compared to the 340% increase for $\sigma = 0.47$ nm can be accounted for only by studying the interaction between side chains. This is the purpose of the next section.

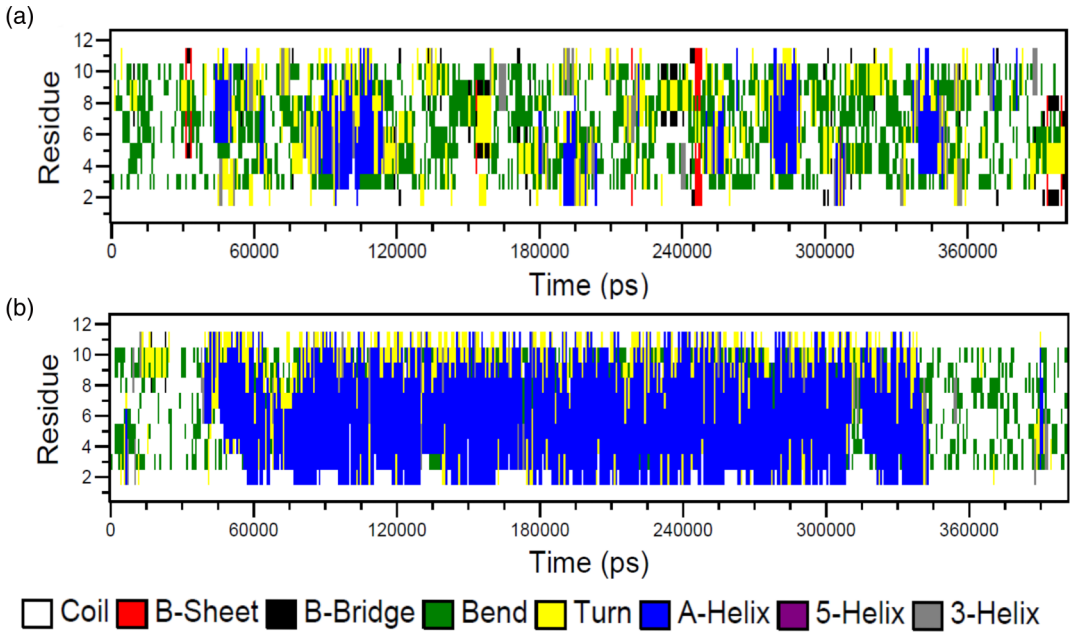

FIG. 3. (Color online) Time evolution of secondary structure content along the amino acid sequence (y axis) for $\epsilon = 1$ kJ/mol. Panels (a) and (b) correspond to $\sigma = 0.37$ nm and 0.47 nm, respectively.

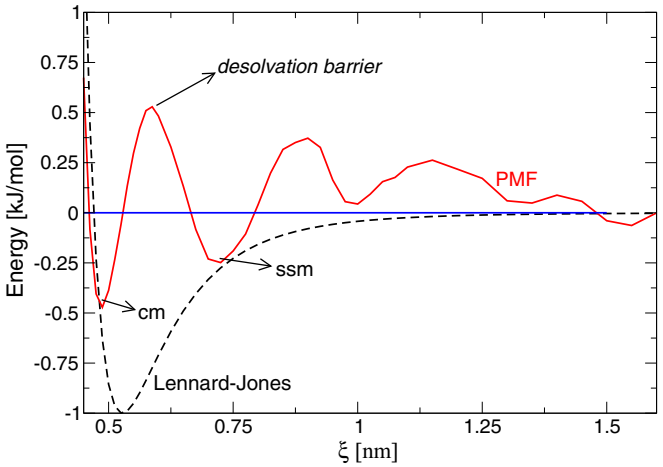

FIG. 4. (Color online) Potential of mean force between methane-like particles and C_β–C_β LJ interaction using $\epsilon = 1.0$ kJ/mol and $\sigma = 0.47$ nm.

C. Methane-like dimers

In order to explain the propensity of α-helix formation in our simulations, we note that for a fixed ϵ, simulations differ in the σ parameter of the C_β–C_β LJ potential. This accounts for different effective potentials between side chains of the peptide. Here, we assume that the effective interaction between side chains (–CH_3 groups) can be approximated by the PMF between two methane-like (CH_4) molecules in solution. Main contributions to this PMF are the direct LJ interactions between C_β atoms and entropic contributions of surrounding water molecules. LJ interactions between carbon atoms are favorable over a wide range of distances (see Fig. 4) whereas the effective PMF between methane molecules is negative only for well-defined positions corresponding to "contact minimum" (CM) and "solvent separated minimum" (SSM); see Fig. 4. As a consequence, the effective potential between side chains can promote a particular secondary structure only if CM and SSM distances are consistent with side-chain distances of this particular structure. Moreover, the difference between CM and SSM positions is $\sim d_w$, where d_w is the diameter of one water molecule. For distances between these two minima, water cannot be accommodated easily between the two methane molecules. This is known as desolvation, which accounts for positive PMF values. Desolvation has been related to cooperative effects [38,64,65] in protein folding as well as its rate-limiting process [40,66].

In Fig. 5(a) we show PMF for the interaction of methane-like molecules that mimic side chains in our polyalanine simulations. To understand how CM and SSM affect α-helix formation, we show in Fig. 5(b) distributions of C_β–C_β distances when peptides are in an helical conformation for our 9-mer and 12-mer simulations [67]. Two prominent peaks emerge at 0.54 nm and 0.72 nm. The first peak at $r = 0.54$ nm is the result of interactions between residues $i - i + 1$ (0.529 nm for a perfect α-helix) and $i - i + 3$ (0.548 nm for a perfect α-helix); see Figs. 5(c)–5(e). These two interneighbor distances appear as a single peak due to thermal fluctuations.

The distance corresponding to the first peak is projected onto the different PMF using a dotted line in Fig. 5(a). The

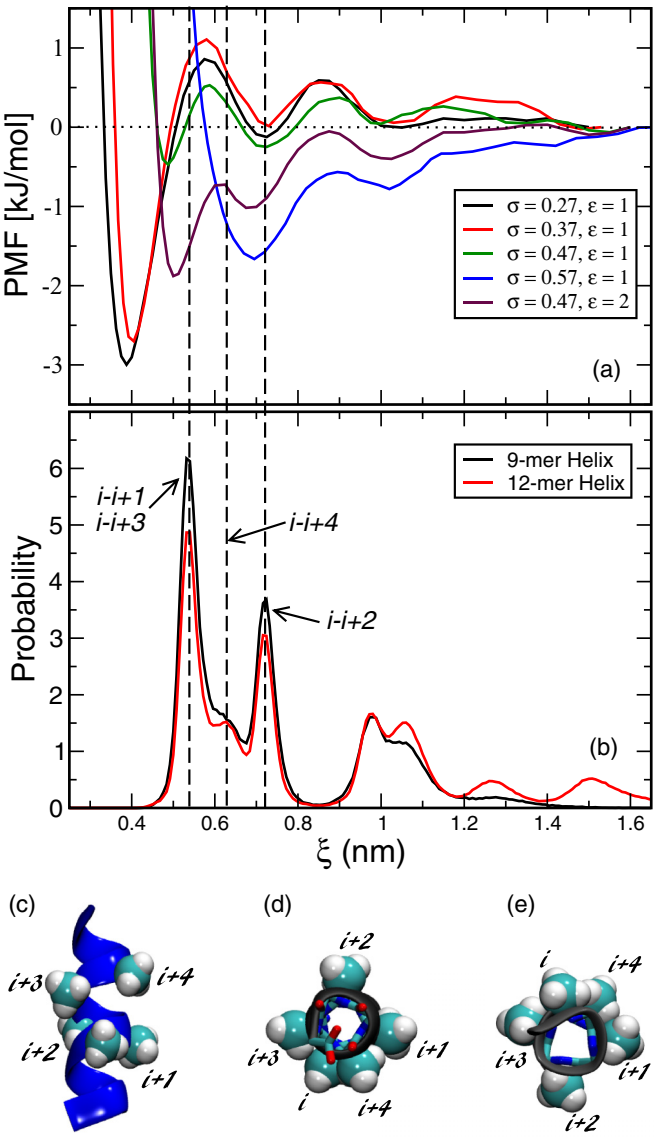

FIG. 5. (Color online) Top: (a) The potential of mean force between two methane-like molecules with different values of the C_β-C_β LJ σ parameter ($\epsilon_{C_\beta-C_\beta} = 1.0$ kJ/mol), solvated in aqueous solution, as a function of the distance between these two central atoms. (b) The normalized distribution of the distance between the C_β atoms in α-helical conformations in 9-mer ($\sigma = 0.47$ nm and $\epsilon = 2.0$ kJ/mol) and 12-mer ($\sigma = 0.47$ nm and $\epsilon = 1.0$ kJ/mol) peptides. The frames of the trajectories in an α-helical conformation were determined by a RMSD (with respect to a perfect helix) cutoff value of 0.12 nm which corresponds to the location of the first minimum of the RMSD histogram. Bottom: Representation of an ideal α-helical structure viewed from (c) the side, (d) C-terminal, and (e) N-terminal (c).

first peak contributes with a positive term to the energy of the system for most of the LJ parameters studied here. It implies that side chains of $i - i + 1$ and $i - i + 3$ residue pairs contribute to increase the energy of the system when α-helices are formed. The exception being $\sigma = 0.47$ nm where the first peak distance is close to the global minimum of the PMF. Accordingly, simulations using $\sigma = 0.47$ nm show the largest α-helical content; see Fig. 2 and Table I. For $\sigma = 0.27$ nm and

$\sigma = 0.37$ nm, the first peak in the distribution of the C_β–C_β distances falls within the desolvation barrier. As a result, $i - i + 1$ and $i - i + 3$ neighbors contribute unfavorably to α-helices, which could explain the low helical content in the corresponding simulations in Fig. 2. Furthermore, for $\sigma = 0.57$ nm the position of the first peak in Fig. 5(b) corresponds to hard-core repulsion in the PMF. This steric clash is very important because in this case the formation of any helical structure is completely destroyed.

The distribution of C_β–C_β distances shown in Fig. 5(b) also displays a shoulder (or a small maximum) at $r = 0.63$ nm, due to $i - i + 4$ neighbors. For $\sigma < 0.57$ nm, intensities of the different PMF at $r = 0.63$ nm fall within the desolvation barrier, and thus $i - i + 4$ neighbors are not likely to contribute favorably to α-helix formation. For $\sigma = 0.57$ nm, $i - i + 4$ neighbors contribute favorably to α-helix formation. However, as mentioned previously, this value of σ cannot accommodate $i - i + 3$ and $i - i + 1$ neighbors in an α-helix because of its hard-core repulsion.

The distribution of C_β–C_β distances exhibits a third peak at $r = 0.72$ nm due to $i - i + 2$ neighbors. PMF of methane-like molecules [Fig. 5(a)] at this distance correspond to SSM, and, therefore, they contribute favorably to the formation of α-helices. However, PMF of methane-like particles in pure water [as the ones computed in Fig. 5(a)] are not good models to describe interactions between $i - i + 2$ neighbors because these two residues are at opposites sides of an α-helix [see Figs. 5(c)–5(e)] and, thus, are not separated by water. We speculate that $i - i + 2$ neighbors are not likely to contribute significantly to α-helix formation since direct LJ and electrostatic interactions between these two residues at 0.72 nm are small; see Fig. 5.

To provide a quantitative framework for the observed correlation between the formation of α-helix and the PMF between methane-like molecules, we compute the average energy of side-chain interactions in our eight simulations. Mathematically we define side-chain energies as

$$E_{\text{sidechain}} = \frac{1}{N} \sum_k \sum_{i,j} \text{PMF}(\xi_{ij}), \tag{1}$$

where the first sum is over the N helical frames in the trajectory and the second sum is over all residue pairs i-j in one frame taken without double counting. Figure 6 shows that the effective energy between side chains when the peptide assumes an α-helix conformation correlate with a larger population of this secondary structure. This is valid for both peptide lengths studied here.

IV. CONCLUSION

To study the role of side-chain interactions in α-helix formation, we performed extensive all-atom molecular dynamics simulations of modified polyalanine peptides in explicit water. We varied the distance and depth of the C_β–C_β LJ interaction, and we identified length scales that promote α-helices. Previous studies on the role of side-chain interactions in secondary structure formation were either limited to implicit water model [45,68–70], restrained peptide simulations [22], or did not take into account effects due to different length scales [54].

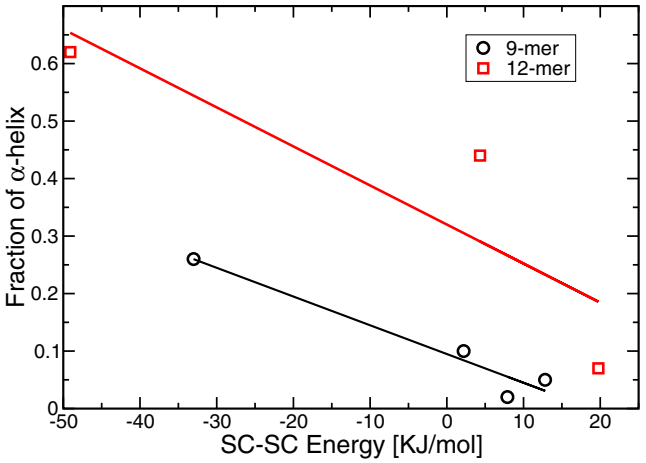

FIG. 6. (Color online) Correlation between side-chain–side-chain (SC-SC) energy and the fraction of α-helix for 9-mer and 12-mer peptides. Lines are a guide to the eye.

To rationalize variations in α-helix content observed in our simulations we computed effective interactions, i.e., PMF between methane-like particles, that mimic side chains in our modified polyalanine peptides. Contact-minimum, desolvation barrier, and solvent-separated minimum of the computed PMF when superposed to distances between $i - i + 1$, $i - i + 3$, and $i - i + 4$ neighbors provided a qualitative explanation for the observed α-helix content in our simulations. In addition, results from our simulations are consistent with previous studies on the role of desolvation barriers on secondary structure formation [45]. Namely, LJ parameters for which the energy barrier emerges at C_β distances corresponding to $i - i + 1$ and $i - i + 3$ neighbors in α-helices are shown to be unfavorable to the formation of these structures.

One implication of our findings is for the development of coarse-grained models. We show the importance of using potentials for side-chain interactions that have solvent effects embedded into them, e.g., desolvation barriers. Our results also highlight limitations of two-bead coarse-grained models to account for side-chain interactions in α-helices. In these structures, beads representing side-chain atoms can form favorable contact only if their size is defined by $\sigma \sim 0.47$ nm. This restricts the variety of amino acids that can be studied with these type of models.

Based on the PMF analysis between methane-like particles, side-chain interactions in polyalanine (which is defined by $\sigma = 0.35$ nm) are unfavorable to α-helices due to the formation of desolvation configuration between side chains. This result is consistent with findings of an early simulation of the interaction between water and an alanine-based α-helix in which water was found to be absent from the space between adjacent C_β groups along the helix axis [71]. Nevertheless, alanine has one of the highest helix-forming tendency among natural amino acids. If side-chain interactions were to play a role in alanine's helix-forming tendency, it would imply that side-chain interactions in unfolded conformations of alanine would be even more unfavorable than in α-helix conformations. However, for this small amino acid it is likely that side-chain interactions are not an important factor

in helix formation [72]. In contrast, side-chain interactions for amino acids defined by $\sigma = 0.47$ nm (this could mimic leucine) are favorable to α-helices since $i - i + 3$ neighbors are in close contact (contact minimum in the PMF). Notice that applied pressure and temperature can change the PMF affecting the stability of side-chain interactions and thereby the propensity for secondary-structure formation [22]. Further investigations are needed to unravel these effects of pressure and temperature.

ACKNOWLEDGMENTS

C.L.D. acknowledges startup funding provided by the New Jersey Institute of Technology. C.L.D. and F.M. are grateful to NJIT's High Performance Computing center for computational resources. R.Z. would like to acknowledge a grant from the Basque Government under the SAIOTEK program, project code S-PE12UN014, as well as a technical and human support provided by SGIker (USED SERVICES) (UPV/EHU, MICINN, GV/EJ, ESF).

[1] C. Branden and J. Tooze, *Introduction to Protein Structure*, 2nd ed. (Garland Publishing, New York, 1999).
[2] T. R. Jahn, O. S. Makin, K. L. Morris, K. E. Marshall, P. Tian, P. Sikorski, and L. C. Serpell, J. Mol. Biol. **395**, 717 (2010).
[3] T. Lührs, C. Ritter, M. Adrian, D. Riek-Loher, B. Bohrmann, H. Döbeli, D. Schubert, and R. Riek, Proc. Natl. Acad. Sci. USA **102**, 17342 (2005).
[4] M. R. Sawaya, S. Sambashivan, R. Nelson, M. I. Ivanova, S. A. Sievers, M. I. Apostol, M. J. Thompson, M. Balbirnie, J. J. W. Wiltzius, Heather T. McFarlane, A. Ø. Madsen, C. Riekel, and D. Eisenberg, Nature (London) **447**, 453 (2007).
[5] L. Pauling and R. B. Corey, J. Am. Chem. Soc. **72**, 5349 (1950).
[6] L. Pauling and R. B. Corey, Proc. Natl. Acad. Sci. USA **37**, 205 (1951).
[7] L. Pauling and R. B. Corey, Proc. Natl. Acad. Sci. USA **37**, 251 (1951).
[8] W. Kauzmann, Adv. Prot. Chem. **14**, 1 (1959).
[9] K. A. Dill, Biochemistry **29**, 7133 (1990).
[10] W. L. Jorgensen, J. Am. Chem. Soc. **111**, 3770 (1989).
[11] C. Narayanan and C. L. Dias, J. Chem. Phys. **139**, 115103 (2013).
[12] Z. Su and C. L. Dias, J. Phys. Chem. B **118**, 10830 (2014).
[13] J. A. Schellman, Compt. Rend. Trav. Lab. Carlsberg. Sér. Chim. **29**, 230 (1955).
[14] P. Y. Chou and G. D. Fasman, Annu. Rev. Biochem. **47**, 251 (1978).
[15] H. Li, C. Tang, and N. S. Wingreen, Phys. Rev. Lett. **79**, 765 (1997).
[16] P. L. Privalov, CRC Crit. Rev. Biochem. Mol. Bio. **25**, 281 (1990).
[17] R. L. Baldwin, J. Mol. Biol. **371**, 283 (2007).
[18] J. T. Edsall, J. Am. Chem. Soc. **57**, 1506 (1935).
[19] S. Shimizu and H. S. Chan, J. Chem. Phys. **113**, 4683 (2000).
[20] D. Paschek, J. Chem. Phys. **120**, 6674 (2004).
[21] S. Shimizu and H. S. Chan, J. Chem. Phys. **115**, 1414 (2001).
[22] C. L. Dias, Phys. Rev. Lett. **109**, 048104 (2012).
[23] C. L. Dias, T. Ala-Nissila, M. Karttunen, I. Vattulainen, and M. Grant, Phys. Rev. Lett. **100**, 118101 (2008).
[24] J. C. Kendrew, G. Bodo, H. M. Dintzis, T. Parrish, H. Wyckoff, and D. C. Phillips, Nature (London) **181**, 662 (1958).
[25] J. C. Kendrew, R. E. Dickerson, B. E. Strandberg, R. G. Hart, D. R. Davies, D. C. Phillips, and V. C. Shore, Nature (London) **185**, 422 (1960).
[26] C. Tanford, Adv. Protein Chem. **23**, 121 (1968).
[27] N. Lupu-Lotan, A. Yaron, A. Berger, and M. Sela, Biopolymers **3**, 625 (1965).
[28] K. T. O'Neil and W. F. DeGrado, Science **250**, 646 (1990).
[29] S. Padmanabhan, S. Marqusee, T. Ridgeway, T. M. Laue, and R. L. Baldwin, Nature (London) **344**, 268 (1990).
[30] M. Blaber, X. J. Zhang, J. D. Lindstrom, S. D. Pepiot, W. A. Baase, and B. W. Matthews, J. Mol. Biol. **235**, 600 (1994).
[31] G. I. Makhatadze, Adv. Prot. Chem. **72**, 199 (2005).
[32] P. Luo and R. L. Baldwin, Proc. Natl. Acad. Sci. USA **96**, 4930 (1999).
[33] J. M. Richardson, M. M. Lopez, and G. I. Makhatadze, Proc. Natl. Acad. Sci. USA **102**, 1413 (2005).
[34] V. Muñoz and L. Serrano, Nature Struct. Mol. Biol. **1**, 399 (1994).
[35] M. M. Lin, O. F. Mohammed, G. S. Jas, and A. H. Zewail, Proc. Natl. Acad. Sci. USA **108**, 16622 (2011).
[36] O. Collet, and C. Chipot, J. Am. Chem. Soc. **125**, 6573 (2003).
[37] R. L. Baldwin and G. D. Rose, Trends Biochem. Sci. **24**, 26 (1999).
[38] M. S. Cheung, A. E. García, and J. N. Onuchic, Proc. Natl. Acad. Sci. USA **99**, 685 (2002).
[39] H. Chan, Z. Zhang, S. Wallin, and Z. Liu, Annu. Rev. Phys. Chem. **62**, 301 (2011).
[40] J. A. Rank and D. Baker, Protein Sci. **6**, 347 (1997).
[41] G. Hummer, S. Garde, A. E. Garcia, and M. E. Paulaitis, Proc. Natl. Acad. Sci. USA **95**, 1552 (1998).
[42] L. R. Pratt and D. Chandler, J. Chem. Phys. **67**, 3683 (1977).
[43] G. Némethy, Angew. Chem. Int. Ed. **6**, 195 (1967).
[44] G. Némethy and H. A. Scheraga, J. Phys. Chem. **66**, 1773 (1962).
[45] C. L. Dias, M. Karttunen, and H. S. Chan, Phys. Rev. E **84**, 041931 (2011).
[46] W. L. Jorgensen, D. S. Maxwell, and J. Tirado-Rives, J. Am. Chem. Soc. **118**, 11225 (1996).
[47] N. A. McDonald and W. L. Jorgensen, J. Phys. Chem. B **102**, 8049 (1998).
[48] R. C. Rizzo and W. L. Jorgensen, J. Am. Chem. Soc. **121**, 4827 (1999).
[49] G. A. Kaminski, R. A. Friesner, J. Tirado-Rives, and W. L. Jorgensen, J. Phys. Chem. B **105**, 6474 (2001).
[50] W. L. Jorgensen, J. Chandrasekhar, J. D. Madura, R. W. Impey, and M. L. Klein, J. Chem. Phys. **79**, 926 (1983).
[51] S. Miyamoto and P. A. Kollman, J. Comp. Chem. **13**, 952 (1992).
[52] B. Hess, H. Bekker, H. J. C. Berendsen, and J. G. E. M. Fraaije, J. Comp. Chem. **18**, 1463 (1997).
[53] G. Vriend, J. Mol. Graph. **8**, 52 (1990).
[54] R. Zangi, Phys. Rev. E **89**, 012723 (2014).

[55] P. S. Georgoulia and N. M. Glykos, J. Phys. Chem. B **115**, 15221 (2011).
[56] B. Hess, C. Kutzner, D. van der Spoel, and E. Lindahl, J. Chem. Theory Comput. **4**, 435 (2008).
[57] T. Darden, D. York, and L. Pedersen, J. Chem. Phys. **98**, 10089 (1993).
[58] G. Bussi, D. Donadio, and M. Parrinello, J. Chem. Phys. **126**, 014101 (2007).
[59] H. J. C. Berendsen, J. P. M. Postma, W. F. van Gunsteren, A. DiNola, and J. R. Haak, J. Chem. Phys. **81**, 3684 (1984).
[60] P. Soto and R. Zangi, J. Phys. Chem. B **109**, 1281 (2005).
[61] X. Wu and B. R. Brooks, Biophys. J. **86**, 1946 (2004).
[62] F. J. Blanco, M. A. Jimenez, J. Herranz, M. Rico, J. Santoro, and J. L. Nieto, J. Am. Chem. Soc. **115**, 5887 (1993).
[63] J. P. Bernacki and M. M. Regina, Biochemistry **50**, 9200 (2011).
[64] J. Zhang, X. Peng, A. Jonas, and J. Jonas, Biochemistry **34**, 8631 (1995).
[65] Z. Liu and H. Chan, J. Mol. Biol. **349**, 872 (2005).
[66] F. Sheinerman and C. Brooks, J. Mol. Biol. **278**, 439 (1998).
[67] Peptides are defined to be in an α-helical conformation whenever the root-mean-square deviation (RMSD) of backbone atoms relative to an ideal α-helix is smaller than 0.13 nm and 0.12 nm for 9-mer and 12-mer peptides, respectively. These cutoff values for the RMSD correspond to the minimum separating the α-helical peak in the RMSD distribution from other conformations. A similar criteria was used in a previous study [54].
[68] F. Ding, J. M. Borreguero, S. V. Buldyrey, H. E. Stanley, and N. V. Dokholyan, Proteins **53**, 220 (2003).
[69] H. D. Nguyen and C. K. Hall, Biophys. J. **87**, 4122 (2004).
[70] H. D. Nguyen, A. J. Marchut, and C. K. Hall, Protein Sci. **13**, 2909 (2004).
[71] A. E. Garcia, G. Hummer, and D. M. Soumpasis, Proteins **27**, 471 (1997).
[72] S. Marqusee, V. H. Robbins, and R. L. Baldwin, Proc. Natl. Acad. Sci. USA **86**, 5286 (1989).